ISBN: 978-3-95450-231-8 ISSN: 2673-5490 doi: 10.18429/JACoW-IPAC2023-WEPL029

MINI-BETA OPTICS FOR THE EUROPEAN SYNCHROTRON RADIATION FACILITY

S. White, C. Benabderrahmane, J. Chavanne, P. Falaise, S. Lagarde, G. Le Bec,
S. Liuzzo, B. Ogier, R. Versteegen, ESRF, Grenoble, France
P. Raimondi, SLAC, Menlo Park, CA, USA

Abstract

The European Synchrotron Radiation Facility (ESRF) presently operates with the Hybrid Multi-Bend Achromat (HMBA) lattice that features β-functions of 6.9 m and 2.7 m in the horizontal and vertical planes at the center of the straight sections. These are not optimal for a length of in-vacuum undulator of approximately 2 m that is used at ESRF. New optics with reduced β-functions at the center of the straight section were designed to better match the electron and photon beams, allow for a reduction of the in-vacuum undulator gap and increase the brilliance delivered to the beam line. This paper presents the optics design, brilliance calculation and plans for experimental validation at the ESRF.

INTRODUCTION

The ESRF new storage ring (ESRF-EBS) was successfully commissioned in 2020 [1]. The HMBA lattice used for the ESRF-EBS storage ring has allowed to reduce the emittance from 4 nm in the previous Double Bend Achromat (DBA) lattice [2] down to approximately 140 pm with insertion devices (ID) opened [3]. Although this represents a significant gain in brilliance for most beam lines there is still margin for further improvement. The ESRF ID straight sections are approximately 5 m long and they can host either one or two 2 m long undulators located on the side or at the center of the straight. The β-functions are 6.9 m and 2.7 m in the horizontal and vertical planes at the center of the straight sections. The β-function in a straight section varies as:

$$\beta(s) = \beta_0 + \frac{(s - s_0)^2}{\beta_0}, \tag{1}$$

where s is the curvilinear coordinate, β_0 the β-function at the center of the straight section and s_0 the s coordinate at the center of the straight section. For an in-vacuum undulator (IVU) the minimum gap is constrained by the vertical β-function at its edges, where they reach a maximum. This represents the most probable location where particle losses can happen and damage the IVU. The optimal vertical β-function at the center of the straight section is therefore the one that minimizes the vertical β-function at the edge of the IVU. From Eq. (1) and assuming an IVU of length L we can write:

$$\beta(L/2) = \beta_0 + \frac{(L/2)^2}{\beta_0}, \tag{2}$$

$$\frac{\delta\beta(L/2)}{\delta\beta_0} = 1 - \frac{(L/2)^2}{\beta_0^2}. \tag{3}$$

The minimum is found where the derivative cancels and we get:

$$\beta_{y,opt} = \frac{L}{2}. \tag{4}$$

In the horizontal plane the optimal β-function is derived from the matching of the electron and photon beam sizes that maximizes the brilliance and can be approximated to [4]:

$$\beta_{x,opt} = \frac{L}{\pi}. \tag{5}$$

When applied to ESRF-EBS, we can see that in the case of a 5.0 m long straight section equipped with two 2 m long IVUs, the vertical β-function of 2.7 m is not far from optimal. However, for a single undulator at the center of the straight section, the β-function would have to be reduced to 1 m. In the horizontal plane, the β-function is very far from optimal as it was optimized for lifetime and it would have to be reduced to 0.64 m to provide optimum matching. A brilliance upgrade for beam lines using a single IVU at the center of the straight section is proposed using an alternative cell optics with reduced β-functions.

OPTICS DESIGN

Even though the proposed design can be applied to any straight section, the calculations presented in this paper consider modification in ID31 only as foreseen for the experimental validation. The optics layout has to give sufficient flexibility to control the horizontal and vertical β-functions at the center of the straight section independently. This is achieved by adding 2 quadrupoles on either side of the straight section. For simplicity, we have considered standard ESRF-EBS medium gradient quadrupoles. The matching quadrupoles used to restore the boundary conditions extend only up to the strong focusing sextupoles (SF), except for the last one (QF4), so that the $-\mathcal{I}$ transform and periodicity of the linear optics at sextupoles are preserved. Several lattices with varying β_x are proposed. Reducing the β-function only in the vertical plane allows to maintain the horizontal cell phase advance constant and test the reduction of the IVU gaps with optimal lifetime. A reduction in both planes is more challenging and will have a stronger impact on lifetime. The implementation of a bunch lengthening cavity to recover the lifetime [5, 6] could be required to operate these lattices. Figure 1 shows the HMBA standard cell (STD) as presently operated at ESRF on the top plot, a mini-β lattice option with the vertical β-function reduced to 1 m and the horizontal β-function maintained at 6.9 m on the middle plot (MB7) and a mini-β lattice option with the vertical β-function reduced to 1 m and the horizontal β-function reduced to 3 m

ISBN: 978-3-95450-231-8 ISSN: 2673-5490 doi: 10.18429/JACoW-IPAC2023-WEPL029

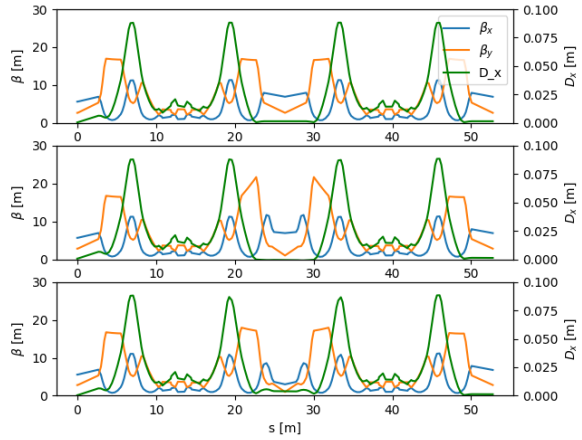

Figure 1: HMBA standard cell (STD, top), mini-β cell with $\beta_{x,y} = (6.9, 1.0)$ m (MB7, middle) and mini-β cell with $\beta_{x,y} = (3.0, 1.0)$ m (MB3, bottom).

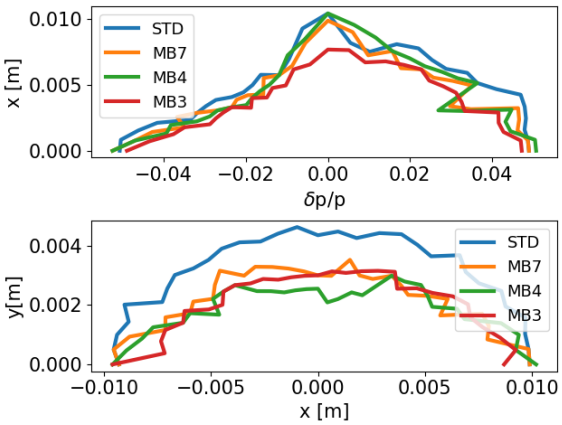

Figure 2: Off-momentum and vertical dynamic apertures for the 3 mini-β and standard HMBA lattices.

on the bottom plot (MB3). An intermediate solution with β_x=4 m was also produced (MB4). For β_x smaller than 3 m the performance degradation is too strong. The strength of the matching quadrupoles for each of these optics is shown in Table 1. The maximum strength allowed in these magnets is 2.89 m^{-1} and a limit of 2.85 m^{-1} was used in the linear optics matching. The limiting factor for all MB optics is the $QD2_{STD}$ strength that is reaching the maximum value.

Table 1: Matching Quadrupoles Strengths for the Mini-β Cells. The QF4 strengths were averaged.

	STD	**MB7**	**MB4**	**MB3**
Units	[m^{-1}]	[m^{-1}]	[m^{-1}]	[m^{-1}]
<$QF4_{STD}$>	2.411	2.372	2.385	2.397
$QD3_{STD}$	-2.389	-1.903	-2.248	-2.382
$QD2_{STD}$	-2.716	-2.850	-2.850	-2.850
$QF1_{STD}$	2.544	1.171	1.867	2.158
$QF1_{MB}$	-	2.234	1.986	1.888
$QD2_{MB}$	-	-1.965	-2.456	-2.655

Reducing the β-functions at the center of the straight section has a significant impact on the lattice: the mini-β cells phase advance is increased by approximately $\pi/2$ due to the smaller β-functions therefore breaking the lattice symmetry. To compensate for this, the optimization steps are the following: i) restore the lattice tune using the standard cells phase advance, ii) fit the chromatic functions to the ones of the symmetric lattice using the sextupoles from the mini-β cells, iii) optimize the lattice working point for dynamic aperture (DA) and lifetime iv) optimize sextupoles using 9 families. This method allows to partially restore the performance. However, the mini-β cells appear as a strong local defect in the lattice, enhance the half-integer resonance and consequently affect off-momentum particles and degrade the lifetime with respect to the standard HMBA lattice. Figure 2 show the dynamic aperture at the injection point without errors for the 3 mini-β lattices and the standard lattice. While the off-momentum dynamic aperture is only mildly affected (MB3 being the worste case) a strong reduction of the vertical dynamic aperture is observed in all cases. These reductions observed even without errors indicate a potential overall performance loss for these lattices. In order to evaluate these lattices in realistic conditions, simulations with errors and corrections were performed. 10 seeds of errors are considered for each lattice and the corrections consist in restoring the closed orbit, coupling and linear optics. For each of the seeds, the on-momentum DA, the Touschek lifetime and injection efficiency (IE) are calculated. The results with and without errors are summarized in Table 2. The results without errors confirm the observations from Fig. 2: both the lifetime and injection efficiency are reduced with respect to the STD lattice. In the best case, the MB7 lattice, the lifetime reduction is of the order of 10 % and there is a 1 % reduce of injection efficiency. This reduction becomes more severe as the horizontal β-function is reduced. The MB lattices appear to be more sensitive to errors and the reduction of lifetime increases to 25 % in the case of the MB7 lattice. The STD lattice performance is the result of a large number iterations of linear and non-linear optimizations on the lattice with errors (the average optimum sextupole set for 10 seeds of errors is used). This could explain its better robustness against errors. Online linear and non-linear lattice optimizations may help recover this loss in performance for the MB lattices. In addition, ongoing developments to increase the lifetime using harmonic cavities [5, 6] and to improve the injection efficiency through a reduction of injection oscillation using fast stripline kickers [7] could provide additional margins for the lattice design.

BRILLIANCE

Figure 3 and Table 3 show the brilliance of the cryogenic permanent magnet undulator (CPMU) installed on the ID31 straight section at the ESRF, computed with the SRW code [8]. With the mini-beta optics, the tuning range of all harmonics is extended to lower energies due to the increased

ISBN: 978-3-95450-231-8 ISSN: 2673-5490 doi: 10.18429/JACoW-IPAC2023-WEPL029

Table 2: Tracking Simulations with Errors and Corrections. The lifetime is calculated for 10 pm vertical emittance and Z/n=0.52 Ω.

	Lifetime	DA(δ_p=0.0)	IE
Units	[h]	[mm]	[%]
Without Errors			
STD	35.3	-9.9	99.1
MB7	32.4	-9.8	98.2
MB4	24.6	-9.9	97.8
MB3	21.3	-9.1	95.4
With Errors			
STD	31.6 ± 1	−9.4 ± 0.4	96.7 ± 1
MB7	23.9 ± 1.6	−9.1 ± 0.7	96.8 ± 1
MB4	21.7 ± 0.7	−9.1 ± 0.3	96.3 ± 1
MB3	17.5 ± 1.5	−7.9 ± 0.7	94.9 ± 1

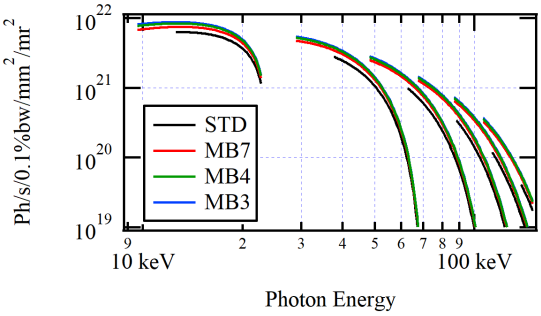

Figure 3: Brilliance curves computed for a CPMU with 14.4 mm period, 2 m long and a peak field of 0.98 T at 5 mm gap (STD) and 1.27 T at 4 mm gap (MB3-7).

undulator deflection at lower gaps. The better matching (Eq. (5)) also increases the brilliance at a given energy and harmonic number. A gain of approximately a factor 2.5 is expected at high energies. More than 80 % of this gain is obtained with the reduction of the vertical β-function. Providing the difficulties maintaining performance compatible with operation when reducing the β-function in both planes it may be more appropriate to restrict the modification to the vertical plane. It should be noted that these results assume a perfect undulator, in reality phase errors may strongly impact the high order harmonics and these results have to be confirmed experimentally in realistic conditions.

Table 3: CPMU Brilliances Computed for the Standard (STD) and the Mini-Beta (MB3-7) Lattices

Energy	STD	MB7	MB4	MB3
[keV]	[10^{21} photons/s/0.1%/mm^2/mrad^2]			
12.6	6.27	7.46	8.35	8.74
50	1.07	2.34	2.56	2.65
100	0.143	0.334	0.363	0.374

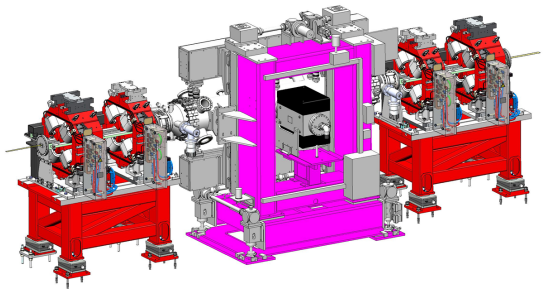

Figure 4: Mini-β test layout for ID31.

ID31 TEST LAYOUT

Experimental validation of the lattice design and the brilliance increase is planned at the ESRF-EBS storage ring. ID31 has a single short period IVU located at the center of the straight section and was therefore chosen for the installation of the test layout. This layout is shown in Fig. 4, where the four additional quadrupoles are in red on either side of the central IVU in purple. Dedicated supports and straight section chambers were purchased to accommodate the 4 additional quadrupoles. Providing this installation is temporary, spare ESRF-EBS magnets were used. The full assembly is now installed and hardware and controls commissioning are ongoing, beam experiments will start shortly after that. The 3 lattices produced allow to gradually reduce the horizontal β-function. It should be noted that the quadrupole layout is sufficiently flexible to generate any intermediate lattices. The main purpose of this test is to demonstrate a reduction of the ID gap to at least 4 mm without significant degradation of injection efficiency or increase of Touschek losses on the ID gap and a lifetime compatible with operation standards. Additional tests with the beamline are planned to measure the gain in brilliance. These results will condition the validation of the concept for operation and the potential need for mitigation measures such has the harmonic cavities or an on-axis injection scheme.

SUMMARY

Mini-β lattices were produced for the ESRF storage ring that would allow to locally increase the brilliance at selected beam lines. Several beam lines have already expressed their interest in this development. Depending on the value of the horizontal β-function at the center of the straight section, the lattice performance degradation can be rather severe and a compromise has to be found between this degradation and the gain in brilliance. A test layout has been installed in the ID31 straight section. This will allow experimental validation of the optics and its compatibility with operation of the storage ring and the beam line IVU. Future studies will include the integration of several such cells in the HMBA lattice and their interplay including the evaluation of cancellation mechanisms.

ISBN: 978-3-95450-231-8 ISSN: 2673-5490 doi: 10.18429/JACoW-IPAC2023-WEPL029

REFERENCES

[1] P. Raimondi *et al.*, "Commissioning of the hybrid multibend achromat lattice at the European Synchrotron Radiation Facility", *Phys. Rev. Accel. Beams*, vol. 24, p. 110701, 2021. doi:10.1103/PhysRevAccelBeams.24.110701

[2] "ESRF foundation phase report (Red book)", ESRF, 1987.

[3] "ESRF upgrade programme phase II", ESRF, 2014.

[4] P. Elleaume, "Lecture on: insertion devices", *CERN accelerator school*, Brunnen, 2003

[5] A. D'Elia, J. Jacob, V. Serrière, and X. W. Zhu, "Design of 4th Harmonic RF Cavities for ESRF-EBS", in *Proc. IPAC'21*, Campinas, Brazil, May 2021, pp. 1031–1033. doi:10.18429/JACoW-IPAC2021-MOPAB332

[6] N. Carmignani, J. Jacob, B. Nash, and S. M. White, "Harmonic RF System for the ESRF EBS", in *Proc. IPAC'17*, Copenhagen, Denmark, May 2017, pp. 3684–3687. doi:10.18429/JACoW-IPAC2017-THPAB003

[7] S. M. White *et al.*, "A Flexible Injection Scheme for the ESRF-EBS", in *Proc. IPAC'21*, Campinas, Brazil, May 2021, pp. 421–424. doi:10.18429/JACoW-IPAC2021-MOPAB116

[8] O. Chubar and P. Elleaume, "Accurate And Efficient Computation Of Synchrotron Radiation In The Near Field Region", in *Proc. EPAC'98*, Stockholm, Sweden, 1998, pp. 1177–1179.